

NOVEL MAGNETIC ALGINATE/HYDROXYAPATITE COMPOSITE WITH HIGH-EFFICIENCY CADMIUM-ADSORPTION PERFORMANCE

NOV KOMPOZIT NA OSNOVI MAGNETNEGA ALGINATA IN HIDROKSIAPATITA Z VELIKO SPOSOBNOSTJO ADSORPCIJE KADMIJA

Xiao Xiao^{2,3}, Jiabei Zhou^{1,*}, Dali Zhou⁴, Liang Li^{2,3}, Yingjiang Wu^{2,3},
Xiang Zhou^{2,3}, Lang Du^{2,3}, Honggen Chen^{2,3}

¹School of Chemical Engineering, Sichuan University, Chengdu 610064, China

²Sichuan Institute of Product Quality Supervision, Inspection and Testing, Chengdu 610100, China

³Chengdu Product Quality Inspection Research Institute Co., Ltd, Chengdu 610100, China

⁴School of Materials Science and Engineering, Sichuan University, Chengdu 610064, China

Prejem rokopisa – received: 2023-06-05; sprejem za objavo – accepted for publication: 2023-12-05

doi:10.17222/mit.2023.927

Heavy-metal pollution (such as Cd(II)) is regarded as a serious environmental problem, posing a great threat to human beings. In this research, a novel water-dispersible magnetic alginate/hydroxyapatite composite with high-efficiency Cd(II) adsorption performance was successfully synthesized by a facile wet-chemical method. The magnetic separation experiment and magnetic property analysis indicate that a magnetic alginate/hydroxyapatite composite can be effectively separated under a magnetic field. The zeta-potential result and dispersity experiment indicate that the lowest zeta-potential is -39.4 mV at pH = 5, and the obtained sample dispersed well in a Cd(II) solution after 120 min. The maximum adsorption capacity of a sample on Cd(II) is 135.3 mg g⁻¹ at pH = 5, and the adsorption of Cd(II) reached equilibrium in 10 min. The adsorption data could be fitted well using the Langmuir model, and the adsorption kinetic follows a pseudo-second-order kinetic model.

Keywords: magnetic alginate/hydroxyapatite composite, Cd(II), water-dispersible adsorbent, magnetic separation

Onesnaženje s težkimi kovinami, kot je na primer dvovalentni kadmij Cd(II), se smatra za enega od najbolj resnih okoljskih problemov, ki ogroža zdravje ljudi. V tem članku avtorji opisujejo raziskavo novega kompozita na osnovi magnetnega alginata in hidroksiapatita z zelo veliko adsorpcijsko sposobnostjo za Cd(II), ki se dobro dispergira v vodi. Avtorji so ga uspešno sintetizirali z enostavno kemijsko metodo. Preizkus magnetnega ločevanja (separacije) in analiza magnetnih lastnosti sta pokazala, da lahko izdelani kompozit učinkovito separiramo s pomočjo magnetnega polja. Rezultati *zeta* potenciala in eksperimenti disperzije so pokazali, da se doseže najnižji *zeta* potencial pri $-39,4$ mV in pH = 5. Pridobljeni vzorec se je dobro dispergiral v raztopini po 120 min. Maksimalna adsorpcijska kapaciteta vzorca na Cd(II) je $135,3$ mg·g⁻¹ pri pH = 5 in adsorpcijsko Cd(II) ravnotežje se vzpostavi po 10 min. Pridobljeni eksperimentalni podatki adsorpcije se lahko dobro opišejo z Langmuirjevim modelom in kinetika adsorpcije dvovalentnega kadmija sledi psevdo kinetičnemu modelu drugega reda.

Ključne besede: kompozit na osnovi magnetnega alginata in hidroksiapatita, dvovalentni kadmij, adsorbent, ki se dispergira v vodi, magnetna separacija

1 INTRODUCTION

Heavy-metal pollution (such as Cd(II)) is regarded as a serious environmental problem, posing a great threat to human beings. The rapid development of industry is considered as the main source of the introduction of heavy-metal ions into soil and ground water.¹ Cd(II) from electroplating, metallurgy and mining industrial sewage is the main heavy-metal pollutant in water and soil ecosystems.² Cd(II) entering the human body could cause an endocrine disorder and a high carcinogenicity, as well as bone fracture and renal dysfunction.³ Therefore, it is very necessary to remediate Cd(II)-polluted soil and water.

Classic accepted techniques used for the removal of Cd(II) from wastewater include adsorption, in-situ solidification chemical precipitation, membrane filtration, and

ion-exchange.⁴⁻⁷ Among the above methods, adsorption was regarded as one of the most promising processes due to its high efficiency, low cost and simplicity of application. For the adsorption technology, adsorbent plays a key role. Traditional adsorbents that were used to remove Cd(II) from wastewater included clay, activated carbon and natural zeolite.⁸⁻¹¹ Rao et al. studied the adsorption of heavy-metal ions in wastewater by kapok-tree-shell-activated carbon, and the results showed that the adsorption capacity of kapok-activated carbon for Cu(II) and Cd(II) reached 20.8 and 19.5 mg/g, respectively.¹² However, these materials had defects, suffering from low efficiency or difficult separation from the treated solution.^{13,14}

HAP and HAP-related materials have been increasingly used to adsorb Cd(II) due to their high adsorption capacity, low water solubility, high chemical stability and low cost.¹⁵⁻¹⁷ Although the HAP has high capacity of Cd(II) adsorption, it is difficult to separate from solution.

*Corresponding author's e-mail:
zjb@scu.edu.cn (Jiabei Zhou)

For such an adsorbent, it is necessary to apply an efficient method of purification that involves materials that can be recycled and does not generate secondary waste.¹⁸

The traditional separation technologies such as filtration, sedimentation and centrifugation are unsuitable or inefficient methods to recover HAP from a liquid phase. To overcome the above problems, magnetic adsorbents are considered owing to the efficient and fast separation from the liquid phase by a magnetic field.¹⁹ Recently, a new water-dispersible magnetic "fluid" adsorbent (suspensions with adsorbents behave like fluid) has been reported with the advantages of low surface potential, fast adsorption rate and easy separation.²⁰ For this, the HAP-related water-dispersible magnetic adsorbent needs to be rationally designed.

In this work, a novel water-dispersible magnetic alginate/hydroxyapatite composite (magnetic alginate/hydroxyapatite composite, M-ALG/HAP) was synthesized as a high-efficiency and easily separable Cd(II) adsorbent. M-ALG/HAP as Cd(II) adsorbent had magnetically separable properties, a high specific surface, a low zeta-potential and was well dispersed in an aqueous solution. The obtained M-ALG/HAP demonstrated a high-efficiency adsorption performance. The adsorption capacity (135.3 mg g^{-1}) of Cd(II) was higher than that for the traditional adsorbent, and the equilibrium time of adsorption was within 10 min.

2 EXPERIMENTAL PART

2.1 Materials

All the chemicals used in this study were of analytical reagent grade. Sodium alginate, calcium chloride ($\text{CaCl}_2 \cdot 2\text{H}_2\text{O}$), sodium dihydrogen phosphate (NaH_2PO_4), sodium hydroxide (NaOH), iron(II) chloride tetrahydrate ($\text{FeCl}_2 \cdot 4\text{H}_2\text{O}$), iron(III) chloride hexahydrate ($\text{FeCl}_3 \cdot 6\text{H}_2\text{O}$), Cd(II) chloride ($\text{CdCl}_2 \cdot 2.5\text{H}_2\text{O}$) and hydrochloric acid (HCl) were from Chengdu Kelong Chemical Co. Ltd. (Sichuan, China).

Before synthesizing M-ALG/HAP, the 2-M NaOH, 0.6-M NaH_2PO_4 and 1-M CaCl_2 solution were prepared for standby. The M-ALG/HAP were synthesized via a wet chemical method. 0.64 g sodium alginate was added to 180 mL of ultrapure water, and stirred for 6 h to obtain a light-yellow sodium alginate solution. Sequentially, 1-M CaCl_2 (8 mL) and 0.6-M NaH_2PO_4 (8 mL) were added dropwise into the sodium alginate solution, then the pH of the solution was adjusted to 13 with 2-M NaOH solution, aged for 20 h to a white suspension. Under nitrogen atmosphere, the FeCl_2 and FeCl_3 mixed solution was drop-wise added to the suspension, stirred for 1.5 h with 75°C , aged 1 day, centrifuged, washed with water three times, and freeze-dried to obtain the M-ALG/HAP sample. For comparison, the pure HAP was synthesized by the coprecipitation method.

2.2 Characterization

The chemical structure and phase composition of M-ALG/HAP were analyzed by FT-IR (Nicolet 6700), XPS (EscaLab 250Xi) and XRD (Shimadzu XRD-6100). The zeta potentials of the M-ALG/HAP in Cd(II) solution were measured by Zetasizer Nano (Malvern Instrument). The morphology of the sample was characterized by SEM (FEI Inspect F50). The BET-specific surface area and pore size distribution were measured by an Automated Specific surface area and Porosity Analyzer (ASAP 2020). The magnetic properties of the M-ALG/HAP were measured by a vibrating-sample magnetometer (VSM, Lakeshore 735).

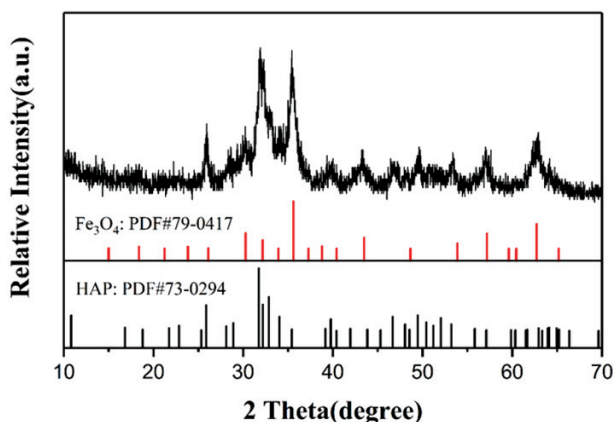
2.3 Cd(II) adsorption test

Considering the ranging of the initial Cd(II) concentration and adsorption time to the adsorption capacity of the M-ALG/HAP, adsorption experiments were carried out using the batch-equilibration technique.

40 mg of M-ALG/HAP sample was added to 100 mL of different concentrations of Cd(II) solution ranging from 25 to 500 mg L^{-1} . The kinetics adsorption experiments were performed at an initial concentration 100 mg L^{-1} , 25°C , pH = 5.0. The Cd(II) concentration of the solution was tested by ICP-AES (IRIS Adv, USA). The amount of Cd(II) adsorbed on the M-ALG/HAP was calculated from the balance relationship.

3 RESULTS AND DISCUSSION

Figure 1 shows the XRD pattern of synthetic M-ALG/HAP. From Figure 1, the diffraction peaks of M-ALG/HAP can be well-indexed as hexagonal HAP (PDF 73-0294), indicating that the sample has hexagonal HAP.²¹ Meanwhile, M-ALG/HAP has an obvious diffraction peak at about $2\theta = 35^\circ$, which corresponds to the characteristic diffraction peak of the (311) crystal plane of Fe_3O_4 (PDF No.70-0417), indicating that the sample has a spinel structure Fe_3O_4 .²² The above XRD results demonstrate that HAP and Fe_3O_4 exist in M-ALG/HAP.



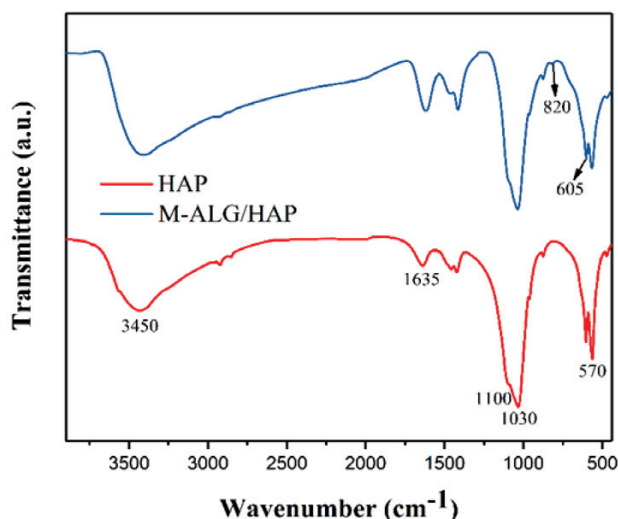


Figure 2: FTIR patterns of synthetic M-ALG/HAP

For the analysis the interaction between the HAP and alginate in M-ALG/HAP composite the FTIR spectra of HAP and the prepared M-ALG/HAP were recorded (Figure 2). The adsorption bands of the HAP and

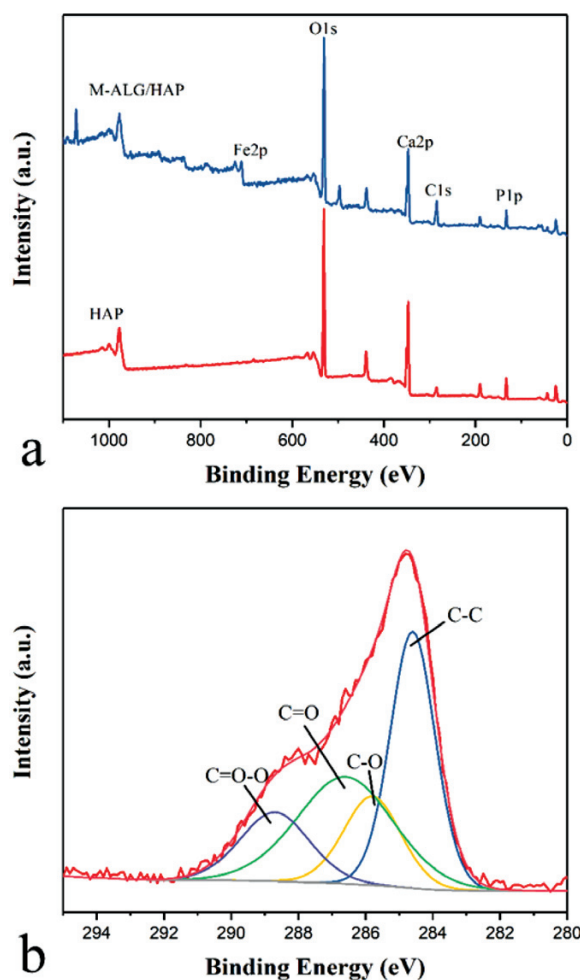


Figure 3: a) XPS survey spectra of M-ALG/HAP, b) C1s spectra of M-ALG/HAP

M-ALG/HAP at 3450 cm^{-1} and 1635 cm^{-1} were attributed to the stretching and bending vibration of the hydroxyl (-OH) groups.²³ The bands at 1100 cm^{-1} and 1030 cm^{-1} were assigned to the PO_4^{3-} asymmetric vibration, and the bands at 605 cm^{-1} and 570 cm^{-1} were attributed to the PO_4^{3-} bending vibration.^{24,25} Compared to the pure HAP, the new adsorption band of M-ALG/HAP at 820 cm^{-1} was attributed to the mannuronic acid (in alginate chemical structure).²⁶ The above results indicate that HAP, alginate and Fe_3O_4 exist in M-ALG/HAP.

Figure 3 shows the XPS spectra of HAP and M-ALG/HAP. From the survey spectra of M-ALG/HAP, there are Ca, P, O, Fe and C elements on the surface of the M-ALG/HAP. The C1s spectra can be divided into the C-C (284.6 eV), C-O (285.8 eV), C=O (286.6 eV) and O-C=O (288.7 eV).²⁷ The peak separation results showed that there were C-C, C-O, C=O and O-C=O in M-ALG/HAP, which was attributed to the existence of these four chemical bonds in the alginate. The above XPS results further proved the existence of HAP, Fe_3O_4 and alginate.

Figure 4 presents the different magnification SEM images of the synthetic M-ALG/HAP. The morphologic investigation shows that the as-prepared M-ALG/HAP had irregular block-like shapes with several hundred nanometers to several micrometers. It can be seen from the high-magnification images that the main part of the block particles is a flocculent structure matrix, which should be alginate. A large number of nearly spherical nanoparticles with a particle size of about 10 nm are coated in and on the surface of the flocculent matrix, which should be HAP and Fe_3O_4 . The EDS results of the M-ALG/HAP are shown in Figure 5. It can be seen from Figure 5 that there are Ca, P, O, Fe and C elements in M-ALG/HAP (Cu is from the Copper grid), which further confirms the existence of a uniform distribution of ALG, HAP and Fe_3O_4 . Using the theoretical analysis of

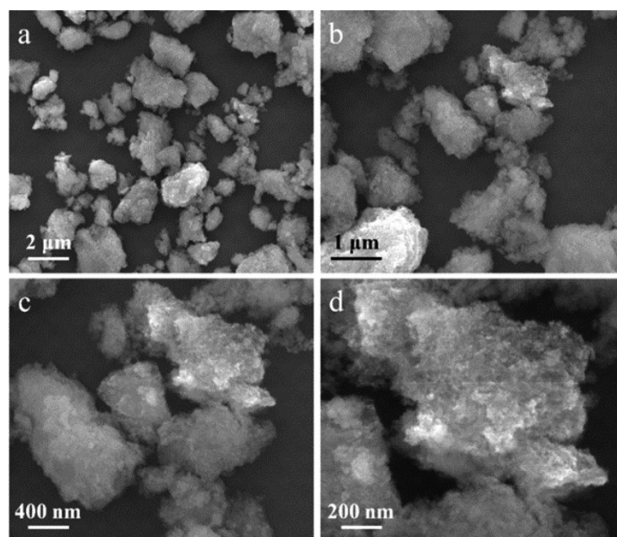


Figure 4: Different magnification SEM images of synthetic M-ALG/HAP

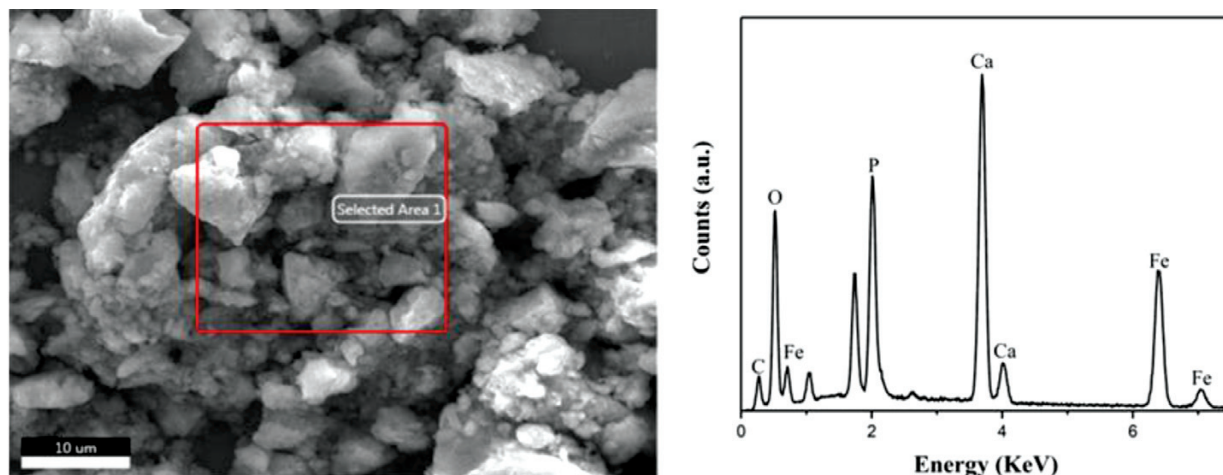


Figure 5: EDS results of the M-ALG/HAP

crystal nucleation and growth, the reason for the growth of the HAP and Fe_3O_4 into nearly spherical nanoparticles is that the large number of $-\text{OH}$ and $-\text{COOH}$ active groups on the ALG molecular chain provide heterogeneous nucleation sites, and the heterogeneous nucleation is easy to homogenize. A large number of crystal nuclei are precipitated explosively, the solute concentration decreases rapidly, and the grain growth rate is slow, so a large number of nearly spherical nanocrystalline particles are formed, and the crystallinity is low.

The VSM result and magnetic separation experiment process of M-ALG/HAP are shown in Figure 6. It can be seen from Figure 6a that the prepared M-ALG/HAP has the greatest saturation magnetization (M_s) of 10.23 emu g^{-1} . Based on this magnetic property of M-ALG/HAP, a magnetic separation experiment was carried out, as shown in Figure 6b. It could be observed that the adsorbent and Cd(II) solution were effectively separated within 1 min, indicating that M-ALG/HAP could be rapidly separated from wastewater in a future practical application.

Figure 7 presents the BJH desorption pore size distribution and N_2 adsorption-desorption isotherm of the prepared M-ALG/HAP. According to the BET result, the specific surface area and average pore size of M-ALG/HAP are $111.7 \text{ m}^2 \text{ g}^{-1}$ and 9.5 nm , respectively.

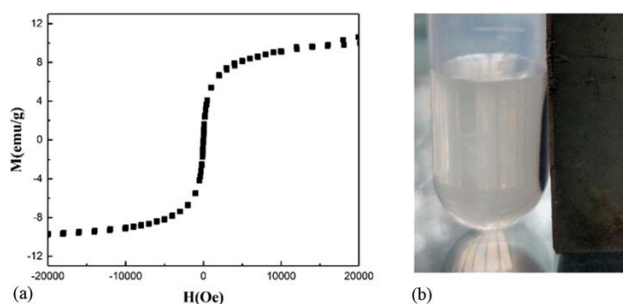


Figure 6: a) VSM analysis result of M-ALG/HAP (298 K), b) separation experiment of M-ALG/HAP from suspension by external magnet (within 1 min)

The Cd(II) adsorption on M-ALG/HAP benefited from a high specific surface area. The N_2 adsorption-desorption isotherm of M-ALG/HAP is type IV with a distinct hysteresis loop ($P/P_0 > 0.4$).¹⁸ This is due to the loose pore structure of ALG, which corresponds to the SEM photos (Figure 4).

Figure 8 shows the dispersibility of the M-ALG/HAP in water, and Figure 9 presents the effect

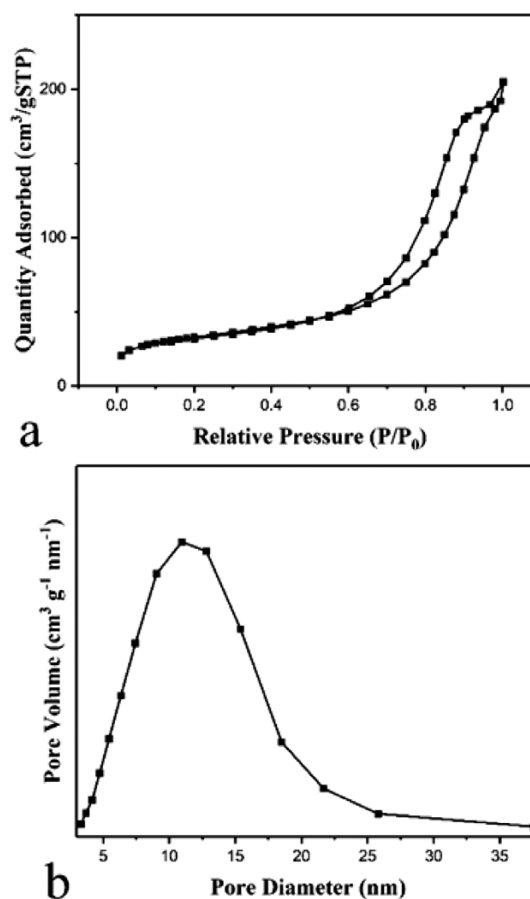


Figure 7: a) N_2 adsorption-desorption isotherm of M-ALG/HAP, b) BJH desorption pore size distribution

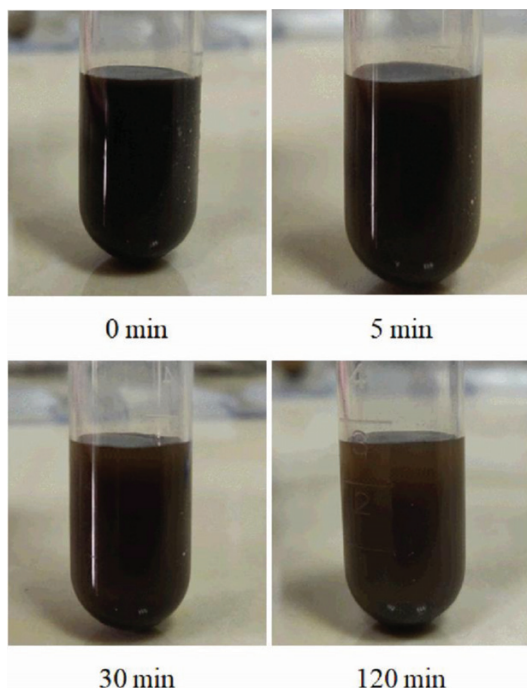


Figure 8: Dispersity of M-ALG/HAP in Cd(II) solution

of different pH values on the zeta-potential of M-ALG/HAP. In the range of pH = 3.0 to 8.0, the zeta-potentials of M-ALG/HAP are all negative, and the negative zeta-potential can promote the adsorption of Cd(II) ions by M-ALG/HAP in an aqueous solution. The zeta-potential of the M-ALG/HAP decreases with the increasing pH from 3.0 to 5.0, the lowest zeta-potential is -39.4 mV at pH = 5, and then become steady when pH = 5.0 to 8.0. Furthermore, the zeta-potential of M-ALG/HAP is lower than that of pure HAP because the ALG structure contains a large number of $-\text{COO}-$ and $-\text{OH}$ functional groups.¹² From **Figure 8**, the obtained M-ALG/HAP dispersed well in Cd(II) solution after 120 min benefiting from the low zeta-potential.

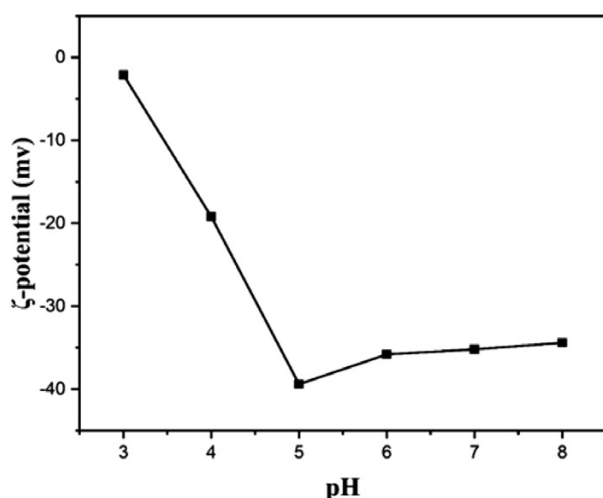


Figure 9: Effect of different pH values on the zeta-potential of M-ALG/HAP

3.2 Adsorption isotherms

The adsorption performance and mechanism of M-ALG/HAP, adsorption isotherms studies over Cd(II) concentration increasing from 25 mg g^{-1} to 500 mg g^{-1} were measured (**Figure 10**). The adsorption experimental data were fitted with the Freundlich and Langmuir models, respectively (Figure 10, fitted parameters in **Table 1**). The Langmuir model has a higher related coefficient ($R^2 = 0.926$) than the Freundlich model. Therefore, the Langmuir model is more suitable for describing the adsorption isotherms of Cd(II) on the M-ALG/HAP, indicating that the adsorption behavior of Cd(II) on M-ALG/HAP is mainly monolayer adsorption.²⁸ This is because the HAP grains in M-ALG/HAP are nearly spherical particles with small particle size (about 10 nm), poor crystallinity and many surface defects and active sites. The maximum theoretical monolayer adsorption capacity (q_{max}) of M-ALG/HAP on Cd(II) is 135.3 mg g^{-1} at pH = 5, which was higher than previously reported for Cd(II) adsorbents.^{29,30}

Table 1: Fitted parameters of adsorption isotherm.

Freundlich model			Langmuir model		
$q_e = KC_e^n$			$q_e = \frac{q_{\text{max}} b C_e}{(1 + b C_e)}$		
R^2	K	n	R^2	q_{max}	b
0.837	76.7	0.112	0.926	135.3	0.78

Note: Where the explanatory note of K , n , b and q_{max} (mg g^{-1}) originate from reference.¹⁸

3.3 Adsorption kinetics

Figure 11 shows the adsorption kinetics of the Cd(II) ion on the M-ALG/HAP. As shown in **Figure 10**, the equilibrium of Cd(II) adsorption could be reached within 10 min, which is faster than on previously reported HAP-related adsorbents.^{16–18} In order to further study the adsorption mechanism, the adsorption experimental results

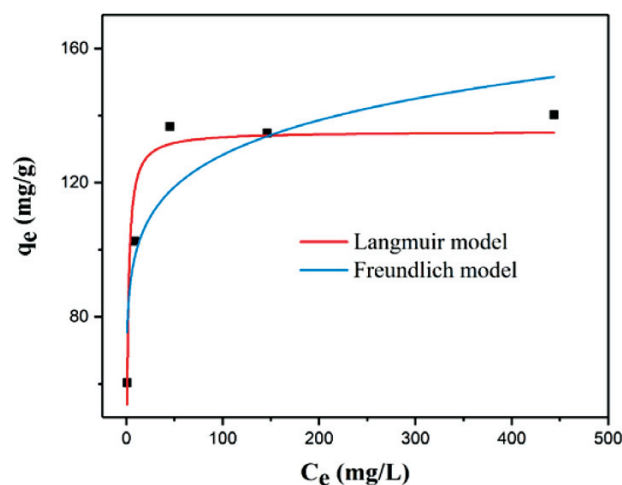


Figure 10: Isotherm curve Cd(II) adsorption on M-ALG/HAP with different concentrations

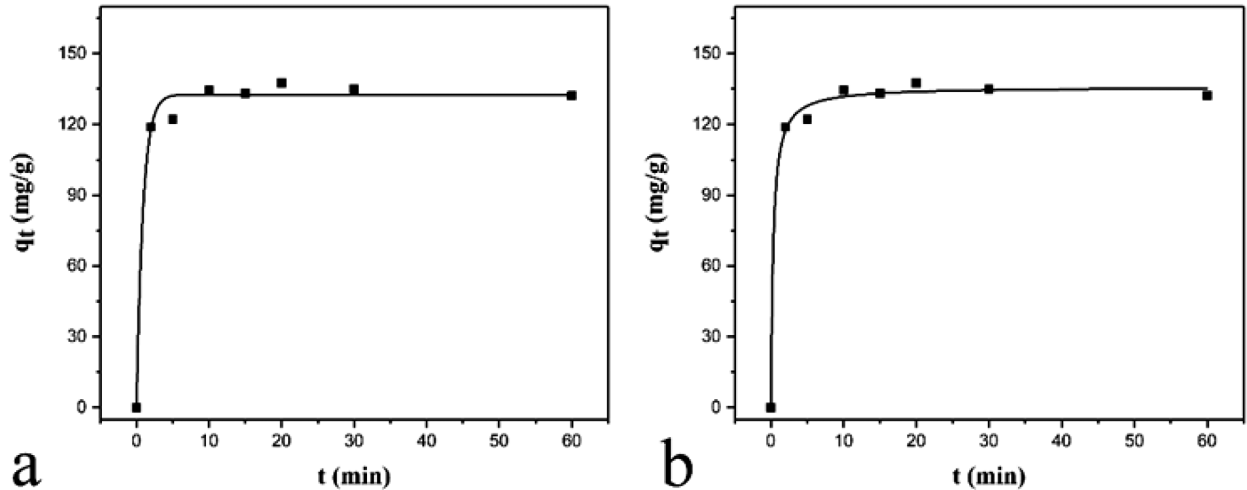


Figure 11: Cd(II) adsorption kinetics (data and fitted curve) on M-ALG/HAP. (a) pseudo-first-order model, (b) pseudo-second-order model

were fitted by the pseudo-second-order model and pseudo-first-order model (**Figure 11**, fitted parameters in **Table 2**).

From **Table 2** and **Figure 11**, the R^2 value of the pseudo-second-order model is higher than those for the pseudo-first-order kinetic model. Thus, the pseudo-second-order model performs a better match between the experimental and theoretical data. The above results reveal that the chemisorption involving valence forces through the exchange or sharing of electrons between Cd(II) ions and adsorbent is the rate-limiting step in the adsorption process of M-ALG/HAP for Cd(II) ion.^{31,32}

From the above adsorption isotherms and adsorption kinetics studies, it is shown that M-ALG/HAP has high-efficiency Cd(II) adsorption performance. This is because M-ALG/HAP has a small grain size, poor crystallinity, many surface defects and active sites, high specific surface area and low zeta-potential.^{18,20} The traditional heavy-metal adsorption process requires a long-term (over 2 h) constant temperature oscillation process. Based on the high-efficiency adsorption performance, water dispersability and magnetic separation ability, the M-ALG/HAP further application as an adsorbent can greatly reduce the oscillation time and simplify the adsorbent separation process. Thus, the heavy-metal adsorption process can be further promoted in the treatment of heavy-metal wastewater.

Table 2: Fitted parameters of adsorption kinetic.

Pseudo-second-order model				Pseudo-frist-order model		
$q_t = \frac{k_2 q_e^2 t}{(1 + k_2 q_e t)}$				$q_t = q_e (1 - e^{-k_1 t})$		
k_2	q_e	h_0	R^2	k_1	q_e	R^2
0.31	135.9	428.2	0.996	1.1	132.7	0.990

Note: Where the explanatory note of q_e (mg g^{-1}), q_t (mg g^{-1}), K_1 (min^{-1}), k_2 ($\text{g mg}^{-1} \text{min}^{-1}$) originate from reference.¹⁸

4 CONCLUSIONS

Heavy-metal pollution from the rapid development of industry is regarded as one of the serious environmental problems, posing a great threat to human beings. In this work, a novel water-dispersible magnetic alginate/hydroxyapatite composite with high-efficiency Cd(II) adsorption performance was successfully synthesized by a facile wet chemical method.

The M-ALG/HAP has a high specific surface area of $111.7 \text{ m}^2 \text{ g}^{-1}$, helping to increase the Cd(II) adsorption capacity. The magnetic separation experiments and VSM analysis reveal M-ALG/HAP can be rapidly separated from the suspension by a magnet. The zeta-potential results and dispersity experiments indicate that the lowest zeta-potential reached -39.4 mV at $\text{pH} = 5$ and the obtained sample dispersed well in a Cd(II) solution after 120 min.

The maximum adsorption capacity of the sample on Cd(II) is 135.3 mg g^{-1} at $\text{pH} = 5$, and the equilibrium of Cd(II) adsorption could be reached within 10 min. The adsorption isotherm could be fitted well by the Langmuir model, indicating that the adsorption behavior of the Cd(II) ion on M-ALG/HAP is mainly monolayer adsorption. The adsorption kinetics follows the pseudo-second-order kinetic model, revealing that the chemisorption involving valence forces through the exchange or sharing of electrons between Cd(II) ions and that the adsorbent is the rate-limiting step in the adsorption process of the M-ALG/HAP for Cd(II) ion.

Acknowledgment

The work was financially sponsored by the Sichuan Province Industry Education Integration Demonstration Project (Chuancaijiao [2022] No.106).

5 REFERENCES

- ¹ L. Wang, H. Gao, M. Wang, J. Xue, Remediation of petroleum-contaminated soil by ball milling and reuse as heavy metal adsorbent, *J. Hazard. Mater.*, 434 (2022) 15, 127305, doi:10.1016/j.jhazmat.2021.127305
- ² C. Y. Gao, C. H. Liang, Y. Yin, L. Y. Du, Thermal activation of serpentine for adsorption of cadmium, *J. Hazard. Mater.*, 329 (2017) 5, 222–229, doi:10.1016/j.jhazmat.2017.01.042
- ³ T. Kikuchi, M. Okazaki, S. D. Kimura, T. Motobayashi, J. Baasansuren, T. Hattori, T. Abe, Suppressive effects of magnesium oxide materials on cadmium uptake and accumulation into rice grains: II: Suppression of cadmium uptake and accumulation into rice grains due to application of magnesium oxide materials, *J. Hazard. Mater.*, 154 (2008) 1–3, 294–299, doi:10.1016/j.jhazmat.2007.10.025
- ⁴ H. Baker, F. Khalil, A study of complexation thermodynamic of humic acid with cadmium (II) and zinc (II) by Schubert's ion-exchange method, *Anal. Chim. Acta.*, 542 (2005) 5–6, 240–248, doi:10.1016/j.wear.2009.12.005
- ⁵ J. Oliva, J. D. Pablo, J. Cortina, J. Gama, G. Ayora, Removal of cadmium, copper, nickel, cobalt and mercury from water by Apatite IITM: Column experiments, *J. Hazard. Mater.*, 194 (2011) 30, 312–323, doi:10.1016/j.jhazmat.2011.07.104
- ⁶ M. Soylak, U. Divrikli, S. Saracoglu, L. Elci, Membrane filtration-atomic absorption spectrometry combination for copper, cobalt, cadmium, lead and chromium in environmental samples, *Environ. Monit. Assess.*, 127 (2007), 169–176, doi:10.1007/s10661-006-9271-0
- ⁷ A. Adg, B. Kpr, C. Vb, A. Hs, Recent trends in the application of modified starch in the adsorption of heavy metals from water: A review, *Carbohydr. Polym.*, 269 (2021) 1, 117763, doi:10.1016/j.carbpol.2021.117763
- ⁸ X. Liang, Y. Zang, Y. Xu, X. Tan, W. Hou, L. Wang, Y. Sun, Sorption of metal cations on layered double hydroxides, *Colloid. Surface. A*, 433 (2013) 2, 122–131, doi:10.1016/j.colsurfa.2013.05.006
- ⁹ S. Guo, P. Jiao, Z. Dan, N. Duan, G. Chen, J. Zhang, Preparation of L-arginine modified magnetic adsorbent by one-step method for removal of Zn(II) and Cd(II) from aqueous solution, *Chem. Eng. J.*, 317 (2017) 1, 999–1011, doi:10.1016/j.cej.2017.02.136
- ¹⁰ A. Shahbazi, H. Younesi, A. Badiei, Functionalized SBA-15 mesoporous silica by melamine-based dendrimer amines for adsorptive characteristics of Pb(II), Cu(II) and Cd(II) heavy metal ions in batch and fixed bed column, *Chem. Eng. J.*, 168 (2011) 2, 505–518, doi:10.1016/j.cej.2010.11.053
- ¹¹ Y. Feng, J. L. Gong, G. M. Zeng, Q. Y. Niu, H. Y. Zhang, C. G. Niu, J. H. Deng, M. Yan, Adsorption of Cd (II) and Zn (II) from aqueous solutions using magnetic hydroxyapatite nanoparticles as adsorbents, *Chem. Eng. J.*, 162 (2010) 2, 487–494, doi:10.1016/j.cej.2010.05.049
- ¹² W. Xu, J. Wang, L. Wang, G. Sheng, J. Liu, H. Yu, X. J. Huang, Enhanced arsenic removal from water by hierarchically porous CeO₂-ZrO₂ nanospheres: Role of surface- and structure-dependent properties, *J. Hazard. Mater.*, 260 (2013) 5, 498–507, doi:10.1016/j.jhazmat.2017.01.042
- ¹³ F. Y. Wang, W. Hui, W. M. Jian, Adsorption of cadmium (II) ions from aqueous solution by a new low-cost adsorbent-Bamboo charcoal, *J. Hazard. Mater.*, 177 (2010) 1–3, 300–306, doi:10.1016/j.jhazmat.2009.12.032
- ¹⁴ M. Dharsana, J. Prakash Arul Jose, Adsorption of lead from contaminated water using biosorbent, *Mater. Tehnol.*, 56 (2022) 2, 171–177, doi:10.17222/mit.2021.352
- ¹⁵ M. Yang, L. Lin, B. Wang, L. Zhang, Y. Jiang, M. Zhao, J. Zeng, H. Chen, Y. Zhang, A facile yet versatile method for adsorption and relayed fluorescent detection of heavy metal ions, *J. Environ. Chem. Eng.*, 9 (2021) 4, 105737, doi:10.1016/j.jece.2021.105737
- ¹⁶ R. Zhu, R. Yu, J. Yao, D. Mao, C. Xing, D. Wang, Removal of Cd²⁺ from aqueous solutions by hydroxyapatite, *Catal. Today.*, 139 (2008) 1–2, 94–99, doi:10.1016/j.cattod.2008.08.011
- ¹⁷ X. H. Zhu, J. Li, J. H. Luo, J. Yang, D. Zheng, Removal of cadmium(II) from aqueous solution by a new adsorbent of fluor-hydroxyapatite composites, *J. Taiwan. Inst. Chem. E.*, 70 (2017), 200–208, doi:10.1016/j.jtice.2016.10.049
- ¹⁸ X. Xiao, L. Yang, D. Zhou, J. Zhou, Y. Tian, C. Song, C. Liu, Magnetic γ -Fe₂O₃/Fe-doped hydroxyapatite nanostructures as high-efficiency cadmium adsorbents, *Colloid. Surface. A*, 555 (2018), 548–557, doi:10.1016/j.colsurfa.2018.07.036
- ¹⁹ J. Y. Tseng, C. Y. Chang, Y. H. Chen, C. F. Chang, P. C. Chiang, Synthesis of micro-size magnetic polymer adsorbent and its application for the removal of Cu(II) ion, *Colloid. Surface. A*, 295 (2007) 1–3, 209–216, doi:10.1016/j.colsurfa.2006.09.001
- ²⁰ H. Ma, S. Pu, Y. Hou, R. Zhu, A. Zinchenko, W. Chu, A highly efficient magnetic chitosan “fluid” adsorbent with a high capacity and fast adsorption kinetics for dyeing wastewater purification, *Chem. Eng. J.*, 345 (2018) 1, 556–565, doi:10.1016/j.cej.2018.03.115
- ²¹ V. Zheltova, A. Vlasova, N. Bobrysheva, I. Abdullin, O. Osmolovskaya, M. Voznesenskiy, O. Osmolovskaya, Fe₃O₄@HAp core-shell nanoparticles as MRI contrast agent: Synthesis, characterization and theoretical and experimental study of shell impact on magnetic properties, *Appl. Surf. Sci.*, 531 (2020) 30, 147352, doi:10.1016/j.apsusc.2020.147352
- ²² S. H. Hosseini, A. Moghimi, M. Moloudi, Magnetic, conductive, and microwave absorption properties of polythiophene nanofibers layered on MnFe₂O₄/Fe₃O₄ core-shell structures, *Mat. Sci. Semicon. Proc.*, 24 (2014), 272–277, doi:10.1016/j.mssp.2014.02.046
- ²³ J. Brownson, M. I. Tejedor-Tejedor, M. A. Anderson, Photoreactive anatase consolidation characterized by ftir spectroscopy, *Chem. Mater.*, 18 (2005) 5, 6304–6310, doi:10.1016/j.jhazmat.2017.01.042
- ²⁴ J. He, K. Zhang, S. Wu, X. Cai, K. Chen, Y. Li, B. Sun, Y. Jia, F. Meng, Z. Jin, L. Kong, J. Liu, Performance of novel hydroxyapatite nanowires in treatment of fluoride contaminated water, *J. Hazard. Mater.*, 303 (2016) 13, 119–130, doi:10.1016/j.jhazmat.2015.10.028
- ²⁵ L. Chen, K. S. Zhang, J. Y. He, W. H. Xu, X. J. Huang, J. H. Liu, Enhanced fluoride removal from water by sulfate-doped hydroxyapatite hierarchical hollow microspheres, *Chem. Eng. J.*, 285 (2016) 5, 616–624, doi:10.1016/j.jhazmat.2017.01.042
- ²⁶ G. Larosa, M. Salerno, J. S. L. Lima, R. M. Meri, M. F. D. Silva, L. B. D. Garvalho, A. Converti, Characterisation of bare and tannase-loaded calcium alginate beads by microscopic, thermogravimetric, FTIR and XRD analyses, *Int. J. Biol. Macromol.*, 115 (2018), 900–906, doi:10.1016/j.ijbiomac.2018.04.138
- ²⁷ S. Liang, Y. Zhou, K. Kang, Y. Zhang, Z. Cai, J. Pan, Synthesis and characterization of porous TiO₂-NS/Pt/GO aerogel: A novel three-dimensional composite with enhanced visible-light photoactivity in degradation of chlortetracycline, *J. Photoch. Photobio. A.*, 346 (2017) 1, 1–9, doi:10.1016/j.jphotochem.2017.05.036
- ²⁸ X. J. Hu, J. S. Wang, Y. G. Liu, X. Li, G. M. Zeng, Z. L. Bao, X. X. Zeng, A. W. Chen, F. Long, Adsorption of chromium (VI) by ethylenediamine-modified cross-linked magnetic chitosan resin: Isotherms, kinetics and thermodynamics, *J. Hazard. Mater.*, 185 (2017) 1, 306–314, doi:10.1016/j.jhazmat.2010.09.034
- ²⁹ M. M. Rao, A. Ramesh, G. P. C. Rao, S. Seshiah, K. Removal of copper and cadmium from the aqueous solutions by activated carbon derived from Ceiba pentandra hulls, *J. Hazard. Mater.*, 129 (2006) 1–3, 123–129, doi:10.1016/j.jhazmat.2017.01.042
- ³⁰ A. Lqbal, M. R. Jan, J. Shah, Recovery of cadmium, lead and nickel from leach solutions of waste electrical and electronic equipment using activated carbon modified with 1-(2-pyridylazo)-2-naphthol, *Hydrometallurgy.*, 201 (2021), 105570, doi:10.1016/j.hydromet.2021.105570
- ³¹ M. S. Chiou, H. Y. Li, Adsorption behavior of reactive dye in aqueous solution on chemical cross-linked chitosan beads, *Chemosphere.*, 50 (2003) 8, 1095–1105, doi:10.1016/S0045-6535(02)00636-7

- ³²L. Uzun, F. Güzel, Rate studies on the adsorption of some dyestuffs and p-nitrophenol by chitosan and monocarboxymethylated(mcm)-chitosan from aqueous solution, J. Hazard. Mater., 118 (2005), 1–3, 141–154, doi:10.1016/j.jhazmat.2004.10.006